Ferdinando Giacco,[1,2] Xueliang Du,[1,2] Vivette D. D'Agati,[3] Ross Milne,[4] Guangzhi Sui,[1,2] Michele Geoffrion,[4] and Michael Brownlee[1,2,5]

Knockdown of Glyoxalase 1 Mimics Diabetic Nephropathy in Nondiabetic Mice

Differences in susceptibility to diabetic nephropathy (DN) between mouse strains with identical levels of hyperglycemia correlate with renal levels of oxidative stress, shown previously to play a central role in the pathogenesis of DN. Susceptibility to DN appears to be genetically determined, but the critical genes have not yet been identified. Overexpression of the enzyme glyoxalase 1 (Glo1), which prevents posttranslational modification of proteins by the glycolysis-derived α-oxoaldehyde, methylglyoxal (MG), prevents hyperglycemia-induced oxidative stress in cultured cells and model organisms. In this study, we show that in nondiabetic mice, knockdown of Glo1 increases to diabetic levels both MG modification of glomerular proteins and oxidative stress, causing alterations in kidney morphology indistinguishable from those caused by diabetes. We also show that in diabetic mice, Glo1 overexpression completely prevents diabetes-induced increases in MG modification of glomerular proteins, increased oxidative stress, and the development of diabetic kidney pathology, despite unchanged levels of diabetic hyperglycemia. Together, these data indicate that Glo1 activity regulates the sensitivity of the kidney to hyperglycemic-induced renal pathology and that alterations in the rate of MG detoxification are sufficient to determine the glycemic set point at which DN occurs.

Diabetes mellitus is the leading cause of end-stage renal disease in the world. In the U.S., the average life expectancy of patients with diabetic end-stage renal failure is only 3 to 4 years, and the 5-year mortality rate for patients with diabetes on hemodialysis is ~70% (1–3). However, only 33–50% of patients with poor glycemic control develop diabetic nephropathy (DN), and a subset of patients with good glycemic control still develop DN (4). Susceptibility to hyperglycemia-induced kidney damage appears to be genetically determined (5,6). Numerous associations have been made between various genetic polymorphisms and the risk of DN (1); however, the molecular mechanisms involved in regulating individual susceptibility to DN are not yet understood.

Five major mechanisms by which hyperglycemia causes microvascular complications have been identified over the past decades. Each of these is activated by a single hyperglycemia-induced process, mitochondrial overproduction of superoxide (7–9). In the kidney, hyperglycemia causes increased reactive oxygen species (ROS) in both glomerular mesangial cells

and proximal tubular cells (10,11). The central pathogenic role of hyperglycemia-induced superoxide in diabetic glomerular injury is directly supported by the observation that overexpression of superoxide dismutase protects 8-month diabetic mice from developing increased fractional mesangial volume, increased glomerular transforming growth factor-β, increased collagen IV, and increased plasma creatinine (12). Kidney levels of superoxide correlate with susceptibility to DN in different mouse strains. Superoxide levels are significantly higher in the kidneys and glomeruli of more DN-susceptible diabetic KK/Ta mice compared with less DN-susceptible diabetic C57BL/6 mice, despite similar levels of hyperglycemia in both strains (13).

We previously showed that overexpression of superoxide dismutase prevented persistent epigenetic changes and altered gene expression induced by transient high glucose. Surprisingly, overexpression of the enzyme glyoxalase 1 (*Glo1*) also prevented these changes (14). Subsequently, we showed that overexpression of the *Caenorhabditis elegans Glo1* ortholog CeGly decreases mitochondrial ROS production in this model organism (15). Consistent with these observations, others have recently reported that overexpression of *Glo1* reduces hyperglycemia-induced oxidative stress in diabetic rats (16) and in cultured mouse renal mesangial cells (17). The major physiologic substrate for GLO1 is methylglyoxal (MG), a highly reactive α-oxoaldehyde formed in cells primarily from the triose phosphate intermediates of glycolysis (18). Together with glyoxalase II and a catalytic amount of glutathione, GLO1 reduces MG to D-lactate. In cells, MG reacts almost exclusively with unprotonated arginine residues to form the major MG-derived epitope MG-H1 [$N\alpha$-acetyl-$N\delta$ (5-hydro-5-methyl)-4-imidazolone]. Diabetes increases levels of MG-H1 in retina, renal glomerulus, and sciatic nerve of rats (19,20).

In this study, we show that in nondiabetic mice, knockdown of *Glo1* increases MG concentration and oxidative stress. In these nondiabetic mice, this causes alterations in kidney morphology identical to those caused by diabetes, independent of the many hormonal and metabolic alterations caused by diabetes. We also show that in diabetic mice, *Glo1* overexpression completely protects from diabetes-induced oxidative stress and kidney pathology, despite diabetic hyperglycemia. These data demonstrate that alterations in the rate of MG detoxification determine the glycemic set point, and thus the susceptibility, to DN.

RESEARCH DESIGN AND METHODS

Mice
Glo1-knockdown (GLO1-KD) mice were generated as previously described (21). Reduced *Glo1* mRNA and protein levels were confirmed by quantitative PCR and Western blot, respectively, as previously described

(22). Heterozygous offspring of the founder had a 50% decrease in kidney GLO1 activity. GLO1-KD mice had body weight, HbA_{1c}, systolic and diastolic blood pressures, and plasma lipid and lipoprotein levels identical to those of wild-type (Wt) control mice (Supplementary Fig. 1).

Glo1-overexpressing (GLO1-Tg) mice were a gift from Dr. Ross Milne (University of Ottawa). In these C57BL/6 mice, cDNA encoding human *Glo1* with an amino terminal c-Myc epitope tag is under the control of the murine preproendothelin promoter. This promoter was chosen because in the kidney, preproendothelin-1 is expressed in tubular epithelium and glomerular mesangial cells, in addition to vascular endothelium (23). In whole kidney, GLO1-Tg mice showed increased protein levels and a twofold increase in activity of GLO1.

To induce diabetes, control (Wt), GLO1-KD, and GLO1-Tg 10-week-old males were injected with streptozotocin (STZ) as previous described (24). STZ-injected mice with glycemia >300 mg/dL were considered diabetic and included in the study. This study conforms to the *Guide for the Care and Use of Laboratory Animals* published by the National Institutes of Health (Publication No. 85-23, revised 1996).

ROS Levels in Kidneys
ROS levels were evaluated by quantifying 3-nitrotyrosine (3-NT) levels by immunoprecipitation–Western blot (IP-WB; n = 5/group). Equal amounts of protein were precleared with an irrelevant antibody to remove proteins that bind immunoglobulins nonspecifically and then subjected to IP with an antibody against 3-NT (mAb Alexis 39B6 [Santa Cruz Biotechnology]), a highly selective and sensitive probe for 3-NT. WB results with this antibody have been corroborated against an independent sensitive and quantitative method, high-performance liquid chromatography (HPLC), which gave comparable results (25,26). IPs were then separated by SDS-PAGE and stained with the same antibody. Intensity of individual bands was measured using the Licor-Odyssey infrared imaging system (Licor).

Twenty-Four–Hour Urine Albumin Measurement
The Albuwell-M kit (Excell, Philadelphia, PA) was used for 24-h urine albumin measurement. Urine was collected for 24 h using metabolic cages, and the total volume was determined. After low-speed centrifugation of aliquots, urine albumin was measured according to the manufacturer's instructions, and total albumin excretion was calculated (n = 15/group).

Histological Analysis
MG modification of proteins was determined by immunohistochemistry using the mouse-on-mouse (M.O.M.) kit (Vector Laboratories, Burlingame, CA). Three-micrometer–thick paraffin sections were deparaffinized and rehydrated in graded ethanols (100 → 50%), followed by

rinsing in distilled H$_2$O. After antigen retrieval, tissue sections were incubated in 3% H$_2$O$_2$ to block endogenous peroxidase activity followed by incubation in avidin/biotin for 15 min. After rinsing with PBS, the tissue sections were blocked with M.O.M. mouse Ig blocking reagent for 1 h and then incubated overnight at 4°C with an HPLC-purified monoclonal anti–MG-H1 antibody prepared as described previously (27) at 1:1,000 dilution. Sections were then incubated with a solution of M.O.M. biotinylated anti-mouse IgG reagent (1:1,000) for 10 min at room temperature. Following application of the avidin-biotin reagent for 5 min at room temperature, slides were incubated in diaminobenzidine, counterstained with hematoxylin, dehydrated, and mounted. Slides were examined under an Olympus light microscope (Olympus) (*n* = 5 mice/group).

Images of 10 glomeruli were analyzed from each mouse. A quantitative analysis of the MG-H1–modified area was performed by using image analysis software from PerkinElmer (Volocity 6.2.1). For each glomerulus, two types of images were imported into Volocity: one image with no primary antibody (negative control) and one image positively stained with both primary and secondary antibody. RGB thresholds were optimized, and a uniform filter was used to remove noise from the system.

Mesangial expansion was quantified in mouse kidneys bivalved and fixed in 10% formalin. Tissues were dehydrated, embedded in paraffin, cut at 3 μm, and stained with periodic acid-Schiff (PAS; Sigma-Aldrich). Light microscopic analysis was performed by surveying the entire cortical area of a PAS-stained slide containing 100–150 glomeruli per section.

The ratio of mesangial area to whole glomerulus was calculated as described previously (28). Light microscopic views after staining with PAS (Sigma-Aldrich) were scanned into a computer, and the quantification of areas of mesangial matrix and glomerulus was performed using a Zeiss microscope and image analysis system (Carl Zeiss AxioVision Release 1.4.1; Carl Zeiss). For each group, 10 glomeruli from each of 15 animals were selected at random on the stained sections.

Electron Microscopy Studies

One-millimeter cubes of mouse kidney cortex were fixed in 2.5% glutaraldehyde, dehydrated, embedded in Epoxy resin, and stained with uranyl acetate and lead citrate. Electron microscopy was performed on a JEOL 1011 electron microscope (Jeol) equipped with digital camera and software for measurement of glomerular basement membrane thickness. Over 80 individual glomerular basement membrane measurements were performed on at least eight glomeruli per mouse (*n* = 15/group).

Statistics

Data are expressed as mean ± SD. ANOVA followed by least significant difference post hoc analysis was used for comparison of different experimental groups. Statistical analyses were performed using PHStat2 software. Statistically significant values are indicated by the following symbols: *$P < 0.05$ versus Wt; and #$P < 0.05$ versus Wt-STZ.

RESULTS

Because MG production is determined by the level of hyperglycemia, whereas MG degradation is determined by GLO1 activity, we first evaluated MG-H1 levels in kidneys from 6-month-old nondiabetic Wt mice, nondiabetic GLO1-KD mice, diabetic Wt mice, and diabetic GLO1-Tg mice. Nondiabetic GLO1-Tg mice and diabetic GLO1-KD mice were also evaluated. MG-H1 levels in kidneys were evaluated by immunohistochemistry using an HPLC-purified anti–MG-H1 antibody. Nondiabetic GLO1-KD (Fig. 1*Ab* and *B*, bar 2) showed increased MG-H1 immunoreactivity in glomerular and tubular compartments compared with nondiabetic Wt mice (Fig. 1*Aa* and *B*, bar 1). In these nondiabetic mice, MG-H1 levels were increased to the same degree as they were in diabetic Wt mice (Fig. 1*Ad* and *B*, bar 4). In contrast, MG-H1 staining in kidneys of diabetic GLO1-Tg mice (Fig. 1*Af* and *B*, bar 6) were the same as in nondiabetic Wt mice. WBs of GLO1-KD mice kidney also showed increased levels of N ε-(carboxyethyl) lysine compared with Wt mice (data not shown). The magnitude of the increase in N ε-(carboxyethyl) lysine from GLO1-KD mice compared with Wt is the same as that observed by Thornalley et al. (29) from STZ diabetic versus Wt kidneys.

ROS levels were evaluated by quantifying 3-NT levels by IP-WB (*n* = 5/group) as described in the RESEARCH DESIGN AND METHODS section. Nondiabetic GLO1-KD (Fig. 1*C*, bar 2) showed a nearly twofold increase in levels of 3-NT compared with nondiabetic Wt mice (Fig. 1*C*, bar 1). In these nondiabetic mice, 3-NT levels were increased to the same degree as they were in diabetic Wt mice (Fig. 1*C*, bar 4). In contrast, 3-NT levels in kidneys of diabetic GLO1-Tg mice (Fig. 1*C*, bar 6) were the same as in nondiabetic Wt mice.

Having determined that knockdown of *Glo1* in nondiabetic mice increased kidney MG-H1 levels and also increased the level of oxidative stress, we next examined albuminuria, an early marker of diabetic kidney dysfunction. Twenty-four–hour albumin excretion was measured in urine of nondiabetic and diabetic Wt, GLO1-KD, and GLO1-Tg mice. Nondiabetic GLO1-KD mice (Fig. 2, bar 2) had an ∼2.5-fold increase in total 24-h urine albumin excretion compared with age-matched nondiabetic Wt mice (Fig. 2, bar 1). Diabetic GLO1-KD mice (Fig. 2, bar 5) had a further 2.5-fold increase in albuminuria compared with nondiabetic GLO1-KD mice and a fivefold increase compared with nondiabetic WT mice. No increase occurred in GLO1-Tg diabetic mice (Fig. 2, bar 6). Albumin excretion in nondiabetic GLO1-Tg mice was reduced 50% compared with nondiabetic WT mice (Fig. 2, bar 3). In Wt diabetic mice, albumin excretion did not increase significantly (Fig. 2, bar 4), consistent with
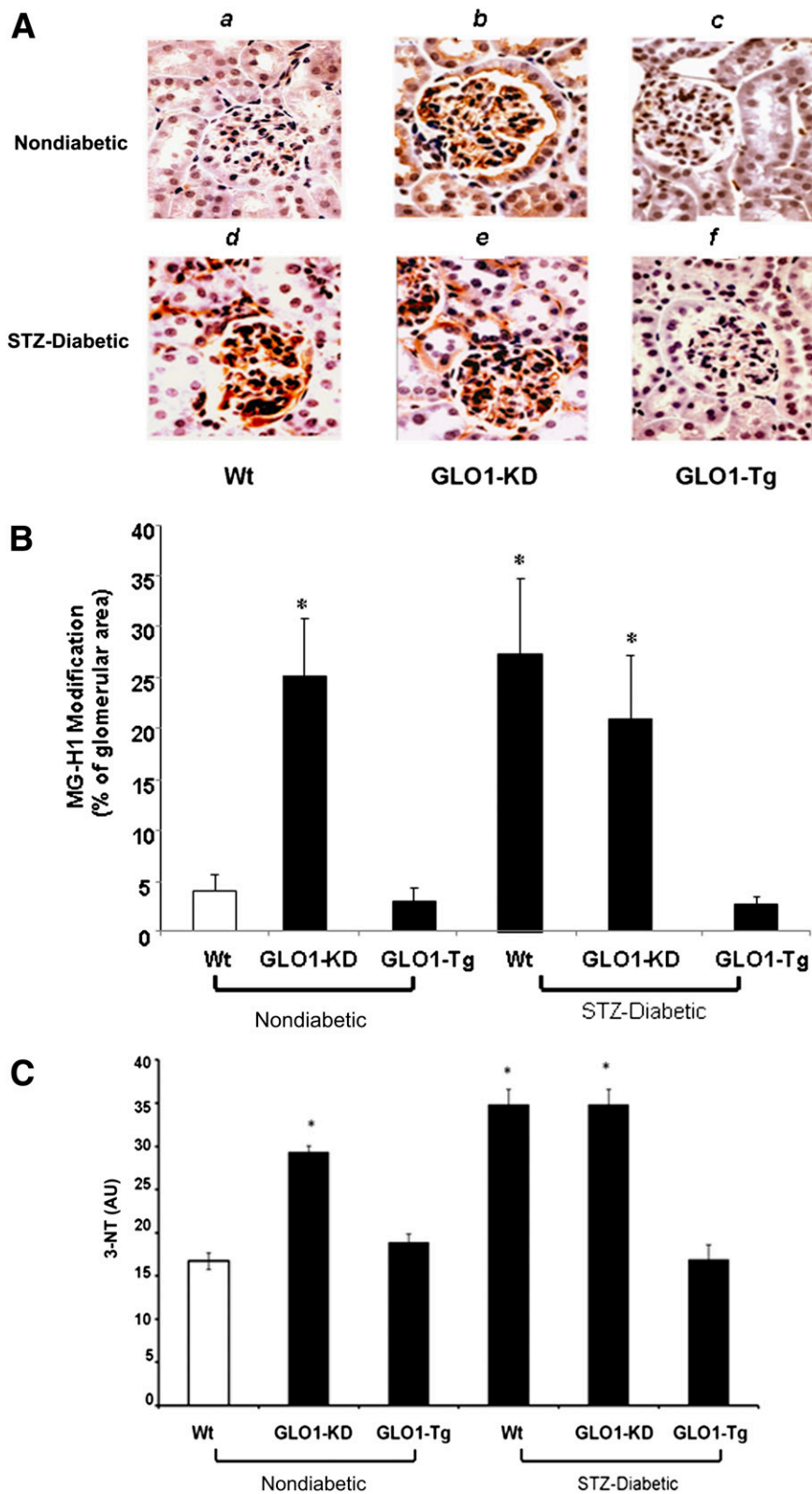
Figure 1—Immunohistochemistry of glomerular MG-modified proteins and kidney oxidative stress ($n = 5$). *A*: Representative photomicrographs of MG-H1 immunostaining from kidneys of nondiabetic (*top panel*) and diabetic (*bottom panel*) Wt (*a,d*), GLO1-KD (*b,e*), and GLO1-Tg (*c,f*) mice. Original magnification ×600. *B*: Quantitation of MG-H1 immunostaining using image analysis software for each group of mice. *C*: Kidney 3-NT levels from nondiabetic and diabetic Wt, GLO1-KD, and GLO1-Tg mice. Data are expressed as mean ± SD (*$P <$ 0.05 vs. Wt, ANOVA). AU, arbitrary units.
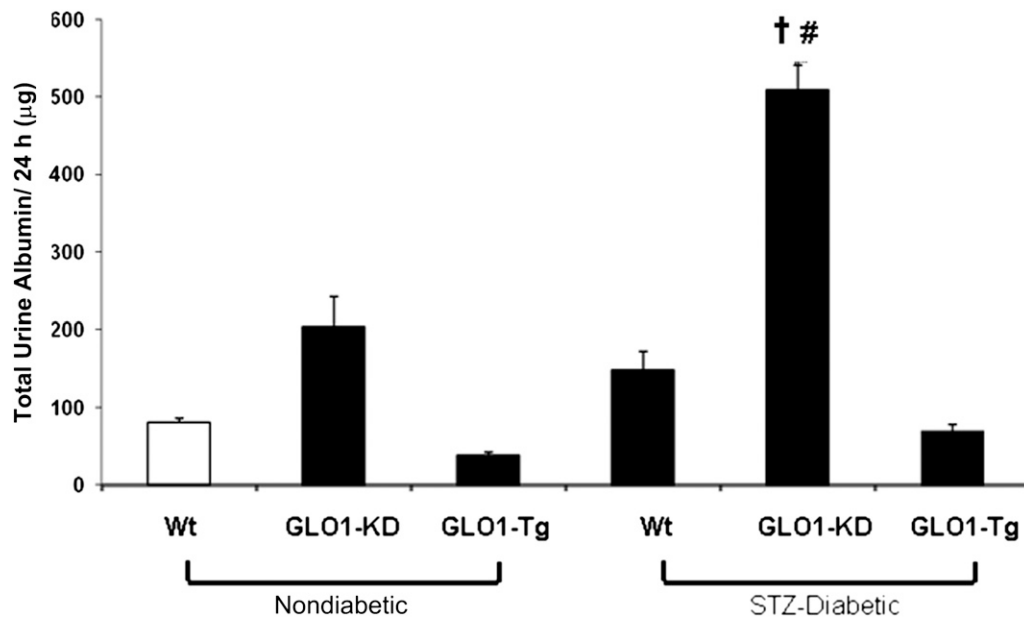
Figure 2—Quantitation of albuminuria in nondiabetic and diabetic Wt, GLO1-KD, and GLO1-Tg mice ($n = 15$). Data are expressed as mean $\pm$ SD ($\dagger P < 0.05$ vs. GLO1-KD; $\#P < 0.05$ vs. STZ-Wt; ANOVA).

previous reports documenting the relative resistance of C57BL/6 mice to diabetes-induced albuminuria (30).

Finally, we assessed the glomerular structural abnormalities that define DN, mesangial expansion, and glomerular basement membrane (GBM) thickness. Fractional mesangial area was evaluated as described in RESEARCH DESIGN AND METHODS (Fig. 3A and B). Nondiabetic GLO1-KD (Fig. 3Ab and B, bar 2) showed a twofold increase in mesangial expansion compared with nondiabetic Wt mice (Fig. 3Aa and B, bar 1). In these nondiabetic mice, mesangial expansion was increased to the same degree as in diabetic Wt mice (Fig. 3Ad and B, bar 4). In contrast, mesangial expansion in kidneys of diabetic GLO1-Tg mice (Fig. 3Af and B, bar 6) was the same as in nondiabetic Wt mice. Fractional mesangial area in nondiabetic GLO1-Tg mice was reduced 50% compared with nondiabetic WT mice (Fig. 3, bar 3).

GBM thickness was evaluated by ultrastructural analysis of electron micrographs as described in RESEARCH DESIGN AND METHODS (Fig. 4). Kidneys from nondiabetic GLO1-KD (Fig. 4Ab and B, bar 2) showed a nearly twofold increase in thickness of the GBM compared with nondiabetic Wt mice (Fig. 4Aa and B, bar 1). In these nondiabetic mice, the degree of increased GBM thickness was identical to that found in diabetic Wt mice (Fig. 4Ad and B, bar 4). In contrast, GBM thickness in kidneys of diabetic GLO1-Tg mice (Fig. 4Af and B, bar 6) was the same as in nondiabetic Wt mice.

To evaluate whether the previously reported alterations in proteasomal activity and promoter histone 3 at lysine 4 (H3K4) monomethylation seen in diabetes contribute to the renal pathological and functional changes

observed in GLO1-KD mice, we measured both proteasomal activity and H3K4 me1 in Wt and GLO1-KD mice. Proteasomal activity was decreased in kidneys of GLO1-KD mice compared with kidneys from Wt mice, similar to what is observed with diabetes (Supplementary Fig. 2A). In contrast, H3K4 monomethylation at the macrophage inflammatory protein 2α promoter, which is increased by hyperglycemia (31), was decreased in kidneys of GLO1-KD mice compared with kidneys from Wt mice (Supplementary Fig. 2B).

DISCUSSION

In the current study, we show for the first time that in nondiabetic C57BL/6 mice, knockdown of *Glo1* increases MG modification of proteins and oxidative stress, causing alterations in kidney morphology indistinguishable from those caused by diabetes. We also show that in diabetic mice, *Glo1* overexpression completely prevents diabetes-induced oxidative stress and kidney pathology, despite unchanged levels of diabetic hyperglycemia.

These data indicate that GLO1 activity regulates the sensitivity of the kidney to hyperglycemic-induced renal pathology. The substrate specificity of *Glo1* is strictly limited to glucose-derived MG and glyoxal. In diabetic tissues, the amount of glyoxal imidazolone adduct on arginine is only 1/50th the amount of the methylgloxal-derived arginine adduct (29), suggesting that MG is quantitatively the major metabolite determining the glycemic set point at which DN occurs. Interestingly, at 6 months, nondiabetic GLO1-Tg mice also had reductions in fractional mesangial volume and albuminuria compared with nondiabetic Wt mice. This observation is
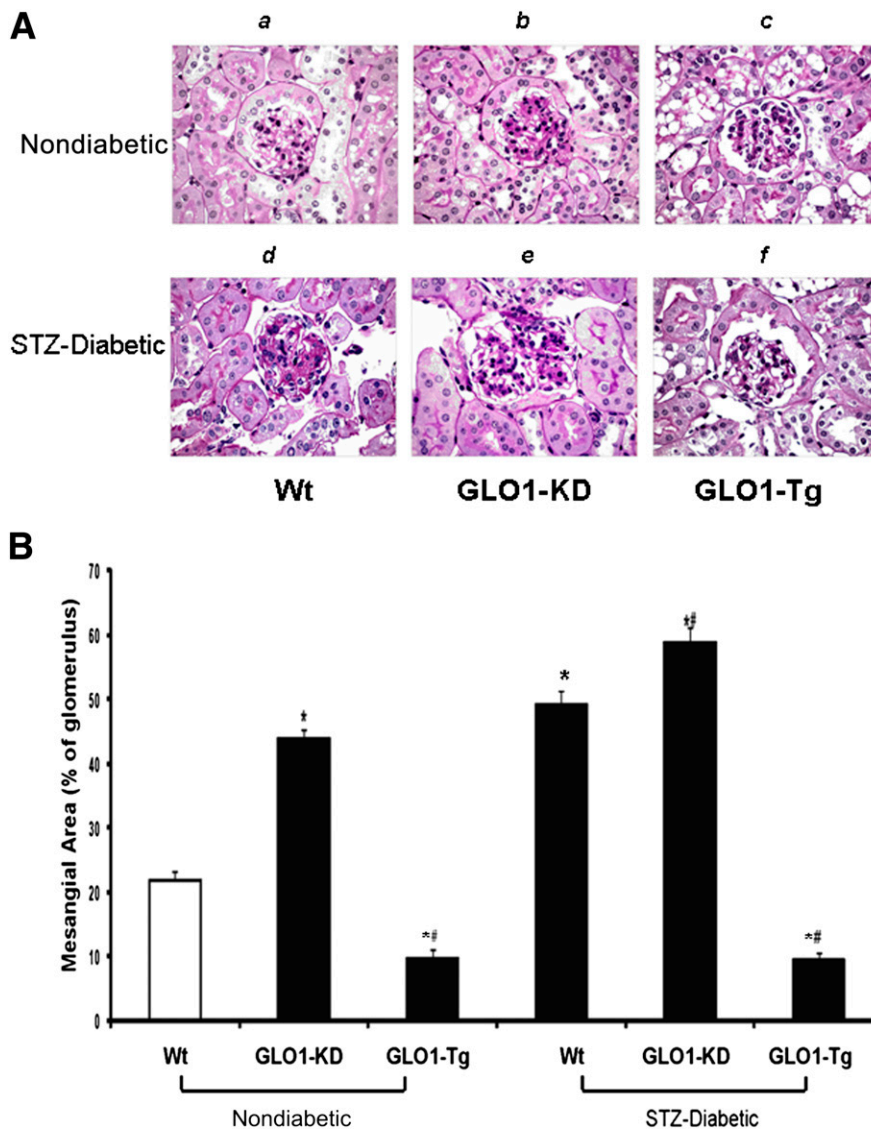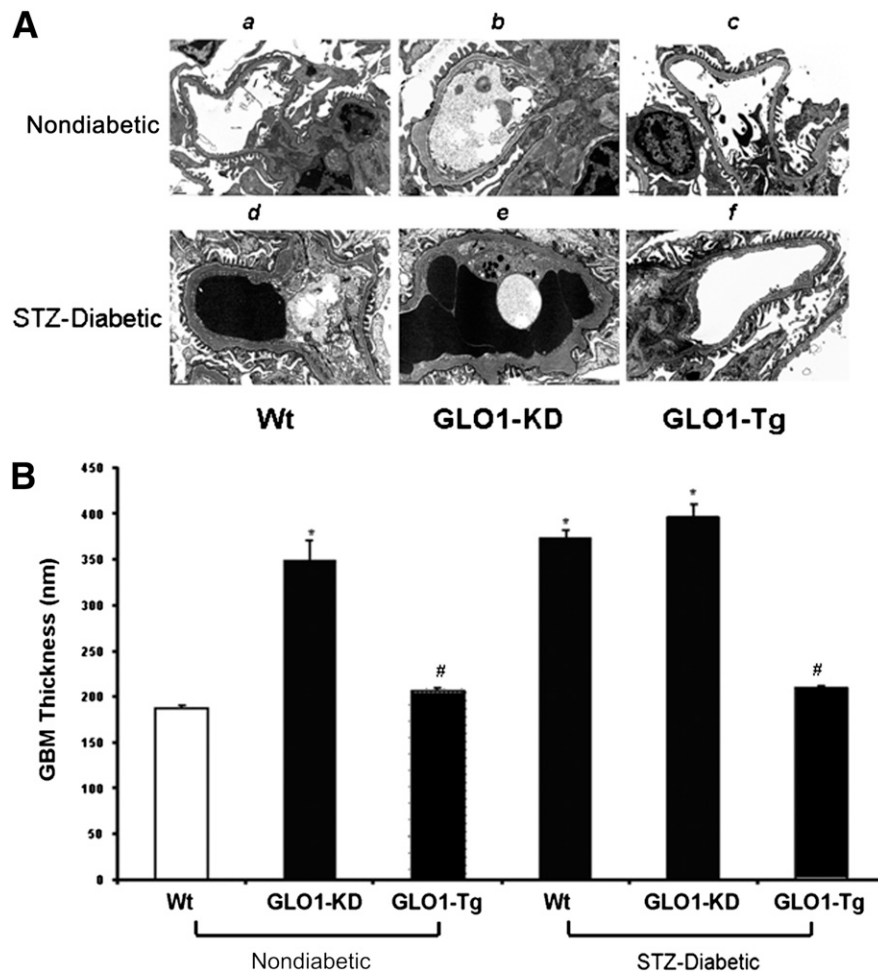
Figure 3—Quantitation of mesangial fractional volume (*n* = 15). *A*: Representative photomicrographs of PAS-stained glomeruli from kidneys of nondiabetic and diabetic Wt (*a,d*), GLO1-KD (*b,e*), and GLO1-Tg (*c,f*) mice. Original magnification ×600. *B*: Quantitation of mesangial fractional volume for each group of mice. Data are expressed as mean ± SD (*P* < 0.05 vs. Wt; #*P* < 0.05 vs. STZ-Wt; ANOVA).

consistent with the report of Ikeda et al. (32) that *Glo1* overexpression significantly decreased age-associated albuminuria and the age-related morphologic changes in nondiabetic rats.

MG levels are increased in diabetic patients and in animal models of diabetes (20). High glucose has been shown to alter the function of several proteins relevant to diabetes complications by increasing their modification by MG. These include the corepressor protein mSin3A, in which MG modification causes increased endothelial expression of angiopoietin 2; the hypoxia-inducible factor 1α–interacting domain of the coactivator protein p300, in which MG modification prevents transcription of hypoxia-inducible factor 1α–dependent genes important in wound healing; the voltage-gated sodium channel Na(v)1.8, in which modification by MG

facilitates nociceptive neuron firing causing hyperalgesia in diabetic rats; and several 20S proteasome subunits, in which modification by MG causes reduced proteasome proteolytic activity (21,33–37).

In the current study, GLO1-KD in STZ-diabetic mice significantly enhanced albuminuria but not the level of MG-H1 or 3-NT, mesangial expansion, or GBM thickness. Since STZ diabetes decreases GLO1 activity in WT mice to the same level as GLO1-KD (data not shown), we speculate that in the glomerulus, increased proteolysis of MG-H1–modified proteins prevents further increase in steady-state levels of MG-H1–modified proteins. Since we found that GLO1-KD in nondiabetic WT mice and STZ-diabetes in WT mice both increased 3-NT to a similar extent, increased proteolysis of MG-H1–modified proteins and its consequences (increased 3-NT and GBM

Figure 4—Measurement of GBM thickness (*n* = 15). *A*: Representative electron micrographs of glomeruli from kidneys of nondiabetic and diabetic Wt (*a,d*), GLO1-KD (*b,e*), and GLO1-Tg mice (*c,f*). Original magnification ×12,000. *B*: Quantitation of GBM thickness. Data are expressed as mean ± SD (*$P \leq 0.05$ vs. Wt; #$P < 0.05$ vs. STZ-Wt; ANOVA).

thickness) would be consistent with this speculation. In contrast, a major determinant of the level of micro-albuminuria is thought to be dysfunction of a tubular high-affinity, low-capacity receptor that lysosomally processes unretrieved filtered albumin (38). We speculate that in tubules, increased proteolysis without a concomitant increase in protein expression causes a decrease in steady-state levels of the protein that regulate albumin reabsorption, further increasing the level of albuminuria.

Changes in MG detoxification rate contribute to hyperglycemia-induced epigenetic changes—increased monomethylation of H3K4—in aortic endothelial cells and mouse aorta (14). However, in GLO1-KD mouse kidney, H3K4 monomethylation at the monocyte chemoattractant protein-2α promoter was reduced. These data suggest that increased monomethylation of H3K4 does not contribute the renal pathological and functional changes observed in GLO1-KD mice.

Overexpression of *Glo1* has been shown to reduce hyperglycemia-induced oxidative stress in diabetic rats

(16) and in cultured mouse renal mesangial cells (17) and to improve hyperglycemia-induced impairment of endothelium-dependent vasorelaxation in mesenteric arteries of diabetic rats (39). *Glo1* overexpression in diabetic rats also reduces retinal neuroglial and vaso-degenerative pathology (40).

However, these studies, like all gene overexpression studies, only demonstrate pharmacologic effects for which relevance to pathogenesis is unknown. Demonstrating that increased endogenous MG levels play a pathogenic role in the development of diabetes complications requires animal models with genetic reduction of *Glo1* expression. Because GLO1-KD mice develop a diabetic-like renal phenotype but do not have diabetes, they provide a unique experimental opportunity to identify pathogenic mechanisms activated by increased MG in nondiabetic mice, independent of the many known mechanisms activated by hyperglycemia.

A number of hyperglycemia-induced mechanisms have been implicated in the pathogenesis of DN. These include

increased flux of glucose and other sugars through the polyol pathway, increased intracellular formation of advanced glycation end products, increased expression of the receptor for advanced glycation end products and its activating ligands, activation of protein kinase C isoforms, and increased activity of the hexosamine pathway. It has also been shown that diabetes causes kidney pathology by affecting the renin–angiotensin aldosterone system, NADPH oxidase activity, transforming growth factor-β, tumor necrosis factor-α, vascular endothelial growth factor-A, Notch, and Janus kinase/signal transducer and activator of transcription pathways (41,42). Whether none, some, or all of these pathways are altered in nondiabetic GLO1-KD mice remains to be investigated. The results of such studies will distinguish between mechanisms that require the abnormal metabolic and hormonal milieu of diabetes and those that are downstream of increased MG concentration.

Oxidative stress plays a pivotal role in hyperglycemia-induced cell damage, altering the activity of a number of hyperglycemia-induced pathogenic mechanisms (9). The level of oxidative stress also correlates with differences in susceptibility to DN in diabetic mice with different genetic backgrounds, but with the same level of hyperglycemia (13). This suggests that ROS levels also regulate individual susceptibility to DN. Our findings show that increasing MG levels increase oxidative stress in nondiabetic mice, while decreasing MG levels abolish hyperglycemia-induced oxidative stress in diabetic mice. These observations are consistent with increased MG levels being the nexus between intracellular hyperglycemia and increased ROS production. In particular, our results are consistent with MG-mediated protein damage being upstream of increased ROS formation. The molecular mechanisms responsible for MG-induced ROS remain to be elucidated. However, it has been shown that mitochondrial proteins from diabetic rat kidney have increased levels of protein modification by MG, consistent with evidence that hyperglycemia-induced ROS originate from mitochondria (8,27,43,44).

Numerous associations have been made between various genetic polymorphisms and the risk of DN (1). However, *Glo1* single nucleotide polymorphisms have not yet been associated with risk of DN. It is now known that copy number variation accounts for as much disease-associated genetic association as single nucleotide polymorphisms, and this has yet to be studied in the context of diabetes complications (45). It is also possible that epigenetic differences affecting *Glo1* transcription exist among individual patients and that tissue-specific variations may exist in transcriptional complex proteins and/or posttranslational modifications that affect GLO1 activity and ROS levels, such as glutathione biosynthetic enzymes and antioxidant enzymes.

In summary, we have shown for the first time that in nondiabetic C57BL/6 mice, knockdown of *Glo1* increases MG modification of proteins and oxidative stress, causing alterations in kidney morphology indistinguishable from those caused by diabetes. We also show that in diabetic mice, *Glo1* overexpression completely prevents diabetes-induced oxidative stress and kidney pathology, despite unchanged levels of diabetic hyperglycemia. These data indicate that *Glo1* activity regulates the sensitivity of the kidney to hyperglycemic-induced renal pathology and that alterations in the rate of MG detoxification are sufficient to determine the glycemic set point at which DN occurs. These findings provide a basis for novel therapeutic approaches to the prevention and treatment of DN.

References

1. Brownlee M, Lloyd AP, Cooper ME, Vinik AI, Nesto RW, Boulton AJM. Complications of diabetes mellitus. In *Williams Textbook of Endocrinology.* 12th ed. Kronenberg HM, Melmed S, Polonsky KS, Larsen PR, Eds. Philadelphia, Elsevier, 2011, p. 1479–1492

2. Centers for Disease Control and Prevention (CDC). Incidence of end-stage renal disease attributed to diabetes among persons with diagnosed diabetes—United States and Puerto Rico, 1996–2007. MMWR Morb Mortal Wkly Rep 2010;59:1361–1366

3. Collins AJ, Foley RN, Herzog C, et al. Excerpts from the US Renal Data System 2009 Annual Data Report. Am J Kidney Dis 2010;55(Suppl. 1):S1–S420, A6–A7

4. Krolewski M, Eggers PW, Warram JH. Magnitude of end-stage renal disease in IDDM: a 35 year follow-up study. Kidney Int 1996;50:2041–2046

5. Quinn M, Angelico MC, Warram JH, Krolewski AS. Familial factors determine the development of diabetic nephropathy in patients with IDDM. Diabetologia 1996;39:940–945

6. Seaquist ER, Goetz FC, Rich S, Barbosa J. Familial clustering of diabetic kidney disease. Evidence for genetic susceptibility to diabetic nephropathy. N Engl J Med 1989;320:1161–1165

7. Brownlee M. Biochemistry and molecular cell biology of diabetic complications. Nature 2001;414:813–820

8. Brownlee M. The pathobiology of diabetic complications: a unifying mechanism. Diabetes 2005;54:1615–1625

9. Nishikawa T, Edelstein D, Du XL, et al. Normalizing mitochondrial superoxide production blocks three pathways of hyperglycaemic damage. Nature 2000;404:787–790

10. Han HJ, Lee YJ, Park SH, Lee JH, Taub M. High glucose-induced oxidative stress inhibits Na+/glucose cotransporter activity in renal proximal tubule cells. Am J Physiol Renal Physiol 2005;288:F988–F996

11. Kiritoshi S, Nishikawa T, Sonoda K, et al. Reactive oxygen species from mitochondria induce cyclooxygenase-2 gene expression in human mesangial cells: potential role in diabetic nephropathy. Diabetes 2003;52: 2570–2577

12. Craven PA, Melhem MF, Phillips SL, DeRubertis FR. Overexpression of Cu2+/Zn2+ superoxide dismutase protects against early diabetic glomerular injury in transgenic mice. Diabetes 2001;50:2114–2125

13. Fujita H, Fujishima H, Chida S, et al. Reduction of renal superoxide dismutase in progressive diabetic nephropathy. J Am Soc Nephrol 2009;20: 1303–1313

14. El-Osta A, Brasacchio D, Yao D, et al. Transient high glucose causes persistent epigenetic changes and altered gene expression during subsequent normoglycemia. J Exp Med 2008;205:2409–2417

15. Morcos M, Du X, Pfisterer F, et al. Glyoxalase-1 prevents mitochondrial protein modification and enhances lifespan in Caenorhabditis elegans. Aging Cell 2008;7:260–269

16. Brouwers O, Niessen PM, Ferreira I, et al. Overexpression of glyoxalase-I reduces hyperglycemia-induced levels of advanced glycation end products and oxidative stress in diabetic rats. J Biol Chem 2011;286:1374–1380

17. Kim KM, Kim YS, Jung DH, Lee J, Kim JS. Increased glyoxalase I levels inhibit accumulation of oxidative stress and an advanced glycation end product in mouse mesangial cells cultured in high glucose. Exp Cell Res 2012;318:152–159

18. Rabbani N, Thornalley PJ. Methylglyoxal, glyoxalase 1 and the dicarbonyl proteome. Amino Acids 2012;42:1133–1142

19. Hammes HP, Du X, Edelstein D, et al. Benfotiamine blocks three major pathways of hyperglycemic damage and prevents experimental diabetic retinopathy. Nat Med 2003;9:294–299

20. Karachalias N, Babaei-Jadidi R, Ahmed N, Thornalley PJ. Accumulation of fructosyl-lysine and advanced glycation end products in the kidney, retina and peripheral nerve of streptozotocin-induced diabetic rats. Biochem Soc Trans 2003;31:1423–1425

21. Queisser MA, Yao D, Geisler S, et al. Hyperglycemia impairs proteasome function by methylglyoxal. Diabetes 2010;59:670–678

22. Yao D, Brownlee M. Hyperglycemia-induced reactive oxygen species increase expression of the receptor for advanced glycation end products (RAGE) and RAGE ligands. Diabetes 2010;59:249–255

23. Slowinski T, Schulz N, Ruschitzka FT, et al. Pattern of prepro-endothelin-1 expression revealed by reporter-gene activity in kidneys of erythropoietin-overexpressing mice. Clin Sci (Lond) 2002;103(Suppl. 48):44S–47S

24. Breyer MD, Böttinger E, Brosius FC 3rd, et al.; AMDCC. Mouse models of diabetic nephropathy. J Am Soc Nephrol 2005;16:27–45

25. Girault I, Karu AE, Schaper M, et al. Immunodetection of 3-nitrotyrosine in the liver of zymosan-treated rats with a new monoclonal antibody: comparison to analysis by HPLC. Free Radic Biol Med 2001;31:1375–1387

26. Franze T, Weller MG, Niessner R, Poschl U. Comparison of nitrotyrosine antibodies and development of immunoassays for the detection of nitrated proteins. Analyst (Lond) 2004;129:589–596

27. Rosca MG, Mustata TG, Kinter MT, et al. Glycation of mitochondrial proteins from diabetic rat kidney is associated with excess superoxide formation. Am J Physiol Renal Physiol 2005;289:F420–F430

28. Wendt TM, Tanji N, Guo J, et al. RAGE drives the development of glomerulosclerosis and implicates podocyte activation in the pathogenesis of diabetic nephropathy. Am J Pathol 2003;162:1123–1137

29. Thornalley PJ, Battah S, Ahmed N, et al. Quantitative screening of advanced glycation endproducts in cellular and extracellular proteins by tandem mass spectrometry. Biochem J 2003;375:581–592

30. Brosius FC 3rd, Alpers CE, Bottinger EP, et al.; Animal Models of Diabetic Complications Consortium. Mouse models of diabetic nephropathy. J Am Soc Nephrol 2009;20:2503–2512

31. Okabe J, Orlowski C, Balcerczyk A, et al. Distinguishing hyperglycemic changes by Set7 in vascular endothelial cells. Circ Res 2012;110:1067–1076

32. Ikeda Y, Inagi R, Miyata T, et al. Glyoxalase I retards renal senescence. Am J Pathol 2011;179:2810–2821

33. Bierhaus A, Fleming T, Stoyanov S, et al. Methylglyoxal modification of Nav1.8 facilitates nociceptive neuron firing and causes hyperalgesia in diabetic neuropathy [published correction appears in Nat Med 2012;18: 1445]. Nat Med 2012;18:926–933

34. Ceradini DJ, Yao D, Grogan RH, et al. Decreasing intracellular superoxide corrects defective ischemia-induced new vessel formation in diabetic mice. J Biol Chem 2008;283:10930–10938

35. Thangarajah H, Vial IN, Grogan RH, et al. HIF-1alpha dysfunction in diabetes. Cell Cycle 2010;9:75–79

36. Thangarajah H, Yao D, Chang EI, et al. The molecular basis for impaired hypoxia-induced VEGF expression in diabetic tissues. Proc Natl Acad Sci USA 2009;106:13505–13510

37. Yao D, Taguchi T, Matsumura T, et al. High glucose increases angiopoietin-2 transcription in microvascular endothelial cells through methylglyoxal modification of mSin3A. J Biol Chem 2007;282:31038–31045

38. Comper WD, Hilliard LM, Nikolic-Paterson DJ, Russo LM. Disease-dependent mechanisms of albuminuria. Am J Physiol Renal Physiol 2008; 295:F1589–F1600

39. Brouwers O, Niessen PM, Haenen G, et al. Hyperglycaemia-induced impairment of endothelium-dependent vasorelaxation in rat mesenteric arteries is mediated by intracellular methylglyoxal levels in a pathway dependent on oxidative stress. Diabetologia 2010;53:989–1000

40. Berner AK, Brouwers O, Pringle R, et al. Protection against methylglyoxal-derived AGEs by regulation of glyoxalase 1 prevents retinal neuroglial and vasodegenerative pathology. Diabetologia 2012;55:845–854

41. Sivaskandarajah GA, Jeansson M, Maezawa Y, Eremina V, Baelde HJ, Quaggin SE. Vegfa protects the glomerular microvasculature in diabetes. Diabetes 2012;61:2958–2966

42. Bonegio R, Susztak K. Notch signaling in diabetic nephropathy. Exp Cell Res 2012;318:986–992

43. Giacco F, Brownlee M. Oxidative stress and diabetic complications. Circ Res 2010;107:1058–1070

44. Rosca MG, Vazquez EJ, Chen Q, Kerner J, Kern TS, Hoppel CL. Oxidation of fatty acids is the source of increased mitochondrial reactive oxygen species production in kidney cortical tubules in early diabetes. Diabetes 2012; 61:2074–2083

45. Rabbani N, Thornalley PJ. Glyoxalase in diabetes, obesity and related disorders. Semin Cell Dev Biol 2011;22:309–317